Inorganica Chimica Acta, 20 (1976) 167 – 181

ICA Review

Molecular Structure, Microstructure, Macrostructure and Properties of Silicon Nitride

H. M. JENNINGS,[1] J. O. EDWARDS,[2]* and M. H. RICHMAN[1]

Division of Engineering,[1] Brown University, Providence, Rhode Island 02912 and Department of Chemistry,[2] Brown University, Providence, Rhode Island 02912, U.S.A.

Received April 9, 1976

Contents

1. Introduction

A chemist is taught and justly follows the precept that an understanding of a pure homogeneous material is a necessary part of his research endeavors. An engineer, however, usually is restricted to using the materials at hand, be they pure or impure, homogeneous or heterogeneous. In the case of the inorganic ceramic silicon nitride Si_3N_4, we have a material which is of tremendous engineering importance yet little is known of its chemistry. It is the purpose of this review to point out what is known about the material, at the molecular level, at the microscopic level and at the macroscopic level, and thus to bring to the attention of inorganic chemists the need for detailed study of the chemical properties of this ceramic. In order to accomplish this goal, we have put some of the engineering data along side of the inorganic facts; we hope that this juxtaposition will integrate the two points of view in a useful way.

There is considerable evidence that silicon nitride can be used in high temperature situations – such as in gas turbine engines – where metal alloys would fail. Together with the good refractory properties of many ceramics, Si_3N_4 has a low coefficient of thermal expansion indicating that large changes in temperature (*e.g.*, from ambient to ~ 1300 °C) would put little stress on the material. Because the efficiency of an engine is closely tied to the highest operating temperature, saving of fuel would be significant if the metal alloy now in use were replaced by the ceramic. The high operating temperature also allows the fuel to combust more completely and thereby reduces pollution.

The samples of Si_3N_4 prepared to date tend to be mixtures of several solid phases, and the percentage of each phase in the samples varies significantly even for samples prepared by a single group using a single technique. It appears that material with optimum potential has not yet been synthesized. Thus the preparation of the silicon nitride ceramic with optimum properties must await the time when inorganic chemists and engineers better understand the reactions by which it is formed and by which it may be decomposed.

2. Chemical Properties

A. Syntheses

A number of methods for preparation of silicon nitride are known. The first references to silicon–nitrogen compounds date back to the middle of the

*To whom correspondence should be addressed.

last century [1]. Both the direct reaction of silicon and nitrogen at very high temperature or the treatment of SiO_2 with alkali amides were claimed, in the early literature, to yield nitrides with the following compositions: SiN, Si_2N_2, Si_3N_4, SiN_2 and sometimes Si_2N_5, SiN_3 and Si_3N. In view of the extreme difficulties encountered by later workers, we feel that the early work on stoichiometry probably is not sufficiently definitive to be taken at face value.

To the best of our knowledge, no other solid compound than Si_3N_4 has been found to exist in the binary system silicon–nitrogen. In principle, however, one could have stoichiometries such as SiN (wherein every silicon would be bonded to three nitrogens and one other silicon).

In one synthesis of Si_3N_4, silica was reduced with carbon in a nitrogen atmosphere at temperatures below 1450 °C [2]. In this reaction, temperature control is important because at higher temperatures silicon carbide can be formed. In another preparation, silica was reduced in a carbon arc furnace and the silicon vapor then reacted with nitrogen [3]. As early as 1910 it was realized that reactions which formed nitrides of silicon were catalyzed by iron [4]. In 1903, Blix and Werbelauer [4] established that the reaction between $SiCl_4$ and NH_3 led to $Si(NH_2)_4$ which, when heated between 1200–1300 °C in a nitrogen atmosphere, produced silicon nitride by a series of deammonations

$$Si(NH_2)_4 \rightarrow Si(NH)_2 \rightarrow Si_2N_3H \rightarrow Si_3N_4$$

At roughly the same time, it was established that elemental silicon and nitrogen do not react at temperatures below 1000 °C [5], and later it was found that at higher temperatures (between 1240 and 1300 °C) a product containing up to 10% nitrogen was produced [6]. These early nitrides were most often formulated as Si_2N_3, SiN or Si_3N_4 and were white or light gray fibrous materials.

In 1910, Si_3C_3N was obtained when silicon was heated in a carbon crucible in an atmosphere of flowing nitrogen [6]. In 1924, Funk [7] reported that the reaction between finely divided silicon and gaseous nitrogen began in the temperature range 1100–1200 °C but that temperatures of at least 1450 °C were necessary in order to obtain Si_3N_4 in good yield. At lower temperatures, some silicon always remained unconverted to the nitride. In 1925 [8], it was established that heating silica and carbon in a nitrogen atmosphere with a few percent hydrogen at 1500 °C produced Si_3N_4 according to the following reaction

$$3SiO_2 + 6C + 2N_2 \xrightarrow{H_2} Si_3N_4 + 6CO$$

and when 10% Fe_2O_3 was added to this charge the reaction temperature could be reduced to 1250–1300 °C. The studies ceased at this point for three decades.

In 1955, Collins and Gerby [9] sparked a renewed interest (now among engineers) in Si_3N_4 when they measured some of its properties. The coefficient of thermal expansion was found to be very low; this fact along with the very high decomposition temperature made it apparent that the material had a potential for high temperature applications such as in gas turbine engines. This led to more extended research on the method of preparing silicon nitride by heating silicon powder in a nitrogen atmosphere at 1300 °C and above. This modernized technique of Parr [10] is the basis of much of the current synthetic technology.

With the recently developed methods for silicon preparation and purification, it is now relatively inexpensive to make silicon nitride in pilot plant quantities. The purity of the ceramic material is, on the other hand, a critical problem. Samples contain greater or lesser amounts of oxygen, iron, carbon and possibly other elements. For reasons to be discussed below, these impurities can have nontrivial effects on the properties of the silicon nitride.

Experiments relating compositions, processing parameters, microstructures and bulk properties have been carried out in our laboratories. The chemical correlations observed are summarized here; the engineering aspects will be discussed elsewhere.

B. Reactions

There have been more studies of the formation of silicon nitride than of its reactions. This is reflected in the review of Wannagat [11] wherein little is said about the material. In the reviews of Croft and Cutler [12], and Edington, Rowcliffe and Henshall [13] emphasis is placed on structure and engineering technology of silicon nitride but the chemical properties are dealt with only in passing.

Silicon nitride exists as a solid in two distinct crystallographic forms (*alpha* and *beta*). Both are very stable with respect to decomposition at temperatures up to at least 1500 °C, and both are formed spontaneously from mixtures of the elements provided the high activation energy barrier to reaction is overcome by high temperature.

The solid is unreactive under normal conditions once a surface layer of silica or oxynitride has been formed. Pieces having both alpha and beta forms present can be oxidized slowly by oxygen or air; tests of oxidizability are usually carried out at 1250 °C over periods of days. There is a suggestion that the *alpha* form may be oxidized more rapidly than the *beta* form [14a], but this is not certain. It has been reported [14a] that the free energy change for the reaction

$$Si_3N_4 + 3O_2 \rightarrow 3SiO_2(\text{B Cris.}) + 2N_2$$

is $-411{,}275$ cal mol^{-1} indicating a large driving force

favoring oxidation and necessitating a protective coating to prevent oxidation.

This above stoichiometry is not the only one reported; apparently some Si_2ON_2 can also be formed in the following manner

$$Si_3N_4 + O_2 \rightarrow Si_2ON_2 + SiO\uparrow + N_2$$

The first stoichiometry predicts a 30% weight gain on oxidation whereas the second predicts a 30% weight loss. The observed change is a small weight gain (often less than 6%). Further the weight gain in 100 hr at 1000 °C is larger than at 1200 °C and this in turn is larger than at 1400 °C. It would be interesting if the two stoichiometries having very different weight characteristics were related to the two stages of oxidation (see below).

The kinetics of oxidation, at least under some conditions follow the parabolic rate law

$$(\Delta W)^2 = K_p \cdot t + C$$

where ΔW represents weight gain, K_p is a rate constant and C is a constant near zero. The activation energy [14b] is about 68 kcal mol^{-1}, which is near to the value reported for oxygen diffusion in SiO_2. The reaction is somewhat faster in oxygen gas than in air. Under some conditions, there are two distinct stages of oxidation, the second much slower than the first.

The reaction of solid pieces with water at 100 °C is very slow. At room temperature pieces hydrolyze slowly in basic solution to give ammonia and silicate solutions; this reaction provides the basis of an analytical procedure wherein released ammonia is titrated by the Kjeldahl determination.

C. Thermodynamics

We would like to be able to say that the thermodynamic properties of silicon nitride were fully worked out, but this is not yet the case. The formation of silicon nitride from the elements is obviously a spontaneous and exothermic reaction in the temperature range from 1100 °C to 1500 °C, because the reaction proceeds well with heat evolution.

Measurements of free energy associated with the reaction

$$3Si(S) + 2N_2(g) = Si_3N_4(S)$$

have been confused by the fact that very often both the *alpha* and *beta* phases are formed simultaneously. It is probable that each of the crystal structures has its own free energy of formation. Detailed crystallographic analysis of the product is not always possible by X-ray methods [21] and is therefore a necessary prerequisite to accurate measurements of the free energy of formation. Table I gives a list of some of the data that has been published. In all cases the entropy change is negative because of the conversion of gas molecules to atoms bound in a solid, making the overall stability of the compound decrease with increasing temperature (*i.e.*, free energy is more negative at lower temperatures). This means that the enthalpy change for this process is always more negative than the free energy change, accounting for the observed exothermicity. The fact that the reaction is observed only at temperatures above 1100 °C is a consequence of a high activation energy or "kinetic barrier" rather than a thermodynamic limitation. Above 1500 °C, the compound is stable in a closed container but can vaporize with decomposition in a vacuum. The decomposition pressure of α-Si_3N_4 has been measured [14c] to be 7.6 mm Hg at 1529 °C.

TABLE I. Free Energy of Formation.

ΔH Kcal/mol	ΔS cal/°K mol	Comment	Reference
−180	−80.4	α and β content unknown	14e
−209	−96.8	forming a mixture of *alpha* and *beta*	16d
−173	−75.3	*alpha* phase formation	14c

The stability of silicon nitride should not be presumed to indicate that it is unreactive. Oxidation by oxygen at high temperatures and basic hydrolysis at low temperatures are known to take place. The non-reactivity of solid samples while in use is fundamentally a consequence of an impervious silicon dioxide or silicon oxynitride coating on the nitride. The reaction of alkaline hydrolysis presumably is a kinetic consequence of the reaction

$$SiO_{2\,(s)} + 2\,OH^- \rightarrow H_2SiO_4^{2-}$$

wherein the protective oxide coat is stripped off by the strongly basic solution.

The thermodynamic data available are subject to some doubt as may be seen in the review of Croft and Cutler [12]. It has not been established to everyone's satisfaction that *alpha* silicon nitride is a true phase in the absence of any oxygen impurity. The *beta* phase apparently is a true phase in the absence of impurities.

3. Fabrication Procedures

Ceramic samples have widely differing strength properties depending on the way in which fabrication (in contradistinction to chemical synthesis) of the specimen is brought about. This is an indirect consequence of the fact that silicon nitride decomposes before it melts (*i.e.*, at lower temperatures than the temperature of fusion) and since it does not exist in the liquid state normal casting procedures are rendered useless.

Further, there are two crystal forms of silicon nitride and one of these exists in two very different macroscopic modifications. Most samples of the ceramic incorporate all three modifications (in variable degrees) plus voids and unreacted silicon. The behavior of a sample depends on all of these and they in turn are dependent on sample preparation. This section contains a brief description of the several techniques used in forming the ceramic.

When preparing silicon nitride using the technique of *reaction bonding*, the first step is to press the silicon powder into the desired shape. The particle size and size distribution of the starting powder are important variables which will influence properties of the product material; some relevant properties are 1) the voidages (again both size and size distribution) in the piece; 2) the density of the sample, and 3) the *alpha* to *beta* ratio (α/β). Compaction of the starting powder is usually accomplished by the technique of cold pressing, by the method of flame spraying (wherein a fine mist is used to form an object), by slip casting or injection molding. The object is then placed into a furnace chamber which is capable of containing a nitrogen atmosphere. The flow rate of nitrogen gas through the chamber is an important variable. Sometimes the chamber is evacuated to remove volatile contaminants before the reaction is initiated, however this has not always been done. The next step, raising the temperature, follows a number of procedures with different groups using different temperature–time programs. The most common technique is to raise the temperature to roughly 1350 °C where it is held for a period of time between one and twenty hours. The temperature is then raised to 1450 °C and held for another period of time between one and twenty hours. Finally, the temperature is lowered and the sample removed. Various heating rates and other holding temperatures are employed depending on the investigator, but strict control of heating rate has not before been considered an important variable. We have, however, considered this a variable of significance and have established the effect of heating rate on the resultant microstructure and properties which increases our control when designing the material for specific properties.

When the sample is removed from the reaction bonding apparatus, the bulk dimensions are unchanged from those of the original silicon compact. This is a great advantage to this technique of forming Si_3N_4 because, once a useful shape is formed with the original powder, little or no further machining is necessary before the object can be used. Another advantage is that good strength at high temperatures is achieved for pieces made by this fabrication technique.

The other fabrication technique for engineering purposes is known as *hot pressing*. Hot-pressed silicon nitride has been most successfully fabricated by mixing a powdered silicon nitride sample (preferably having mostly *alpha* phase) with a few percent MgO. This mixture is then pressed in graphite dies at temperatures above 1700 °C and at pressures of about 250 atmospheres for periods of time from several minutes to an hour. The resulting sample has a density of about 3.1 g cc^{-1}, much higher than the reaction-bonded version which has density of between 2.3 and 2.7 g cc^{-1}. Because of the smaller number of voids and smaller void volumes, the hot-pressed silicon nitride tends to be stronger than reaction-bonded silicon nitride at least at ambient temperatures. The added MgO (and related impurities) in the hot-pressed pieces has a deleterious effect in that creep is enhanced at high temperatures.

Modification of these two basic procedures is possible. The engineering literature now has descriptions of "pyrolytically-deposited silicon nitride" and of "flame spray route reaction-bonded silicon nitride". Silicon compacts to be used in reaction-bonding sequences can now be formed by cold isostatic pressing, slip casting, injection or warm die molding, or even thin film techniques. It seems probable that some new procedure, which has the advantages of both the reaction bonding and hot pressing methods and the disadvantages of neither, can be devised. For example, heating a compacted mixture of powdered silicon nitride and powdered silicon in a stream of nitrogen gas could give a sample with different strength properties than the usual reaction-bonded silicon nitride (this may have been already tried but if so we are not aware of it).

Suffice it to say here that simple formation of silicon nitride from the elements remains a far step away from having a piece of ceramic with desired shape and optimum strength characteristics.

4. Molecular Structure*

A. Crystal Structures

In 1958, Turkdogn, Billo and Tuppet [16a] found that two distinct crystallographic forms of silicon nitride exist. At first it was thought that the form which was designated as *alpha* was a low temperature phase and the other, *beta,* was a high temperature phase. It has since been shown that both phases form under a variety of conditions (including a temperature range between 1150 °C and 1550 °C) and that the concept of high and low temperature phases has

*Attention should be drawn at this point to three reviews. Croft and Cutler [12] published an extensive review (including some material on the chemistry and crystal structure) on work done up to 1973. Messier and Murphy [15] have compiled an annotated bibliography on silicon nitride. A review by Edington *et al.* [13] primarily related to engineering aspects appeared recently.

been difficult to establish because of overriding kinetic effects. This shall be discussed further in a later section. Both forms have hexagonal symmetry and while everyone agrees on the crystal structure of the *beta,* there remains controversy over the detailed structure of the *alpha* form.

Since the *beta* form is better understood it will be discussed first. The unit cell is hexagonal and the lattice parameters are a = 7.608 ± 0.005 Å, c = 2.911 ± 0.001 Å. Figure 1 is a photograph of a model

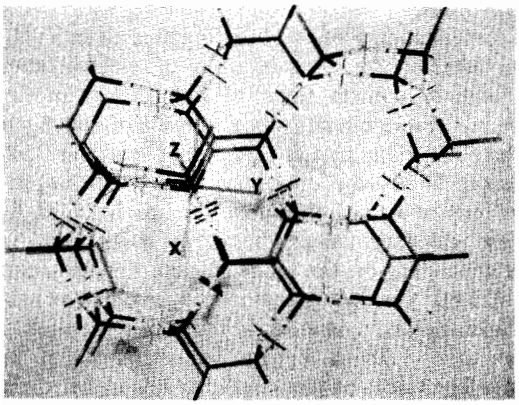

Fig. 1. Model of *beta* phase. Coordinate system labeled x, y, z. Black represents silicon. White represents nitrogen and metal prongs denote the filled p orbitals which enter into *pi* bonding with silicon d orbitals. Grey represents nitrogen but in this case the filled p orbitals are oriented so that only a small amount of *pi* bonding is possible. View of model showing hexagonal symmetry of the tunnels (looking down the z axis).

showing the hexagonal symmetry of the *beta* silicon nitride with each silicon atom at the center of an irregular tetrahedral arrangement of nitrogens and each nitrogen being shared by three of these tetrahedra. This cell contains Si_6N_8. The *beta* structure has been assigned to space group $P6_{3/m}$ [16b] and although there have been minor disagreements as to details, the basic structure has not been contested. In Fig. 2 there are two nitrogens, designated N(2), that occupy the center position of an equilateral triangle of silicon atoms while the other six nitrogens, designated N(1), are located at the centers of 2 less regular triangles of silicon atoms.

As can be seen from Fig. 2 the *beta* structure has hexagonal tunnels in the ⟨0001⟩ direction with an opening of radius 1.5 Å. It is interesting to note, as will be pointed out in the kinetics section, that nitrogen has a Van der Waals radius of 1.5 Å.

The *alpha* modification has been more difficult to characterize. The unit cell has the composition $Si_{12}N_{16}$, and the space group P31c. Table II summarizes the bond lengths reported by two groups [16c, d] of workers having contrasting points of view as to the stoichiometry. The two stoichiometries differ only in the presence or absence of an occasional (but ordered) oxygen. The principal difference between the two structures is that one stoichiometric postulation does not require the presence of oxygen and the other does make this requirement. This question of the presence and the stabilizing effect of oxygen has been the source of controversy as well as of practical suggestions as to approaches to investigators of both hot-pressed and reaction-bonded silicon nitride. The percentage of *alpha,* for instance, might

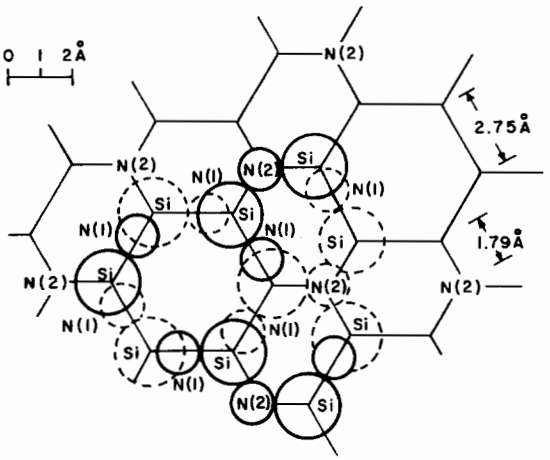

Fig. 2. The atomic arrangement of *beta* silicon nitride. The z direction is perpendicular to the plane of the paper. Solid lines indicate atoms that are located in the plane of the paper. Dotted lines indicate atoms that are located .50z into and out from the plane of the paper. All Si–N(2) bond lengths are 1.745 Å. Si–N(1) bond lengths are divided evenly between 1.730 Å and 1.739 Å. Each silicon atom has three Si–N(1) bonds so that when a particular silicon has two longer and one shorter bond its nearest silicon neighbors have two shorter and one longer bond. The lattice structure is such that this arrangement of Si–N(1) bonds is repeated throughout.

TABLE II. Tetrahedral Bond Lengths and Lattice Parameters for α-Si_3N_4.

	ref. 16a	Wild *et al.* [16b]
Si(1)–N(1)	1.708(15) Å *	1.566–(O_2 SITE)
N(1)	1.775(15)	1.687–(O_2 SITE)
N(2)	1.738(13)	1.795
N(3)	*1.730(6)*	*1.781*
Mean Si(1)–N	1.738	1.707
Si(2)–N(1)	1 763(16)	1.896–(O_2 SITE)
N(2)	1.758(40)	1.893
N(2)	1.700(40)	1.562
N(4)	*1.731(5)*	*1.782*–(Vacancy)
Mean Si(2)–N	1.738	1.783
a	7.766(10)	7.7533(7)
c	5.615(8)	5.6167(8)

*Standard deviation of last significant figures in parenthesis.

well be controlled by simply varying the oxygen content.

It has been found [17, 18] using neuron activation analysis, that at least some forms of *alpha* silicon nitride did not contain sufficient quantities of oxygen to support the idea that oxygen is an integral part of the *alpha* structure. Fig. 3 shows a photograph of a model of this oxygen-free version of *alpha* silicon nitride and examination shows that it is very similar to the *beta* structure except that every basal layer is a mirror image of its adjacent layer. This requires, as is observed, that the *c* parameter be about twice that of the *beta* structure. The *alpha* structure has openings large enough to hold atoms of 1.5 Å radius connected by .7 Å radius passages.

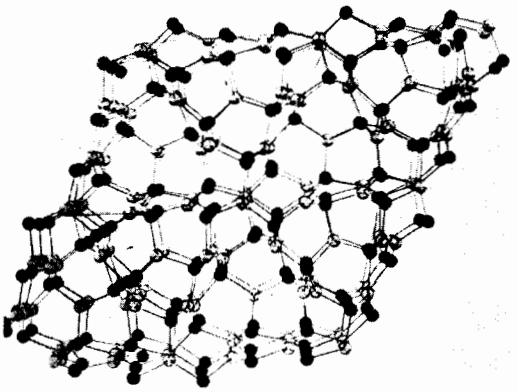

Fig. 3a. Model of *alpha* phase showing hexagonal unit cell.

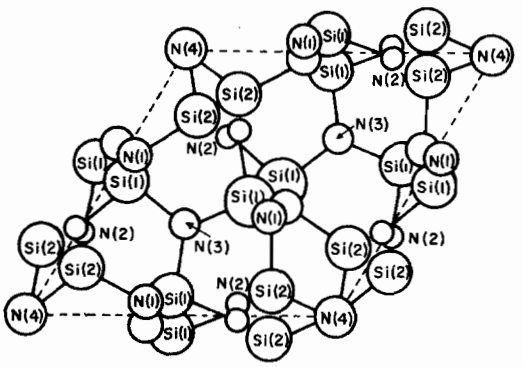

Fig. 3b. Atomic arrangement for *alpha* phase (after Wild, Grieveson, and Jack [16d]).

The oxygenated *alpha* phase [16c] is similar to the above version except that two of every 32 nitrogens are replaced by one oxygen and one silicon position in every 24 is vacant. This oxynitride has a stoichiometry of $Si_{23}N_{30}O$ with oxygens periodically occupying ordered sites as indicated in Table II.

B. Electronic Structures

The valence shell electronic configuration of the silicon atom is $3s^2 3p^2$ and that of nitrogen is $2s^2 2p^3$. Silicon is tetrahedrally coordinated in the elemental solid and most other compounds; this geometry is also seen in both alpha and beta silicon nitride. Nitrogen displays a number of geometries depending on the other atoms attached to it in the compound. It exhibits tetrahedral geometry in ammonium compounds such as NH_4^+ and $N(CH_3)_4^+$, pyramidal geometry in ammonia and most amines, and planar geometry in amides and compounds such as trisilylamine and tris(trimethylsilyl)amine. Nitrogen geometries of the latter two types are found in the silicon nitrides.

An understanding of the bonding present in Si_3N_4 can be attained by consideration of electrostatic, *sigma* and *pi* contributions to bonding in model compounds. From covalent radii, the silicon–nitrogen bond length is estimated as 1.92 Å; application of the Schomaker–Stevenson correction for electronegativity difference brings this down to about 1.80 Å. As these calculations are based on tables having entries dependent on the mode of determination the value of 1.80 Å is only a reasonable first approximation. Nevertheless, it is unlikely that the value should be less than 1.78 Å before consideration of *pi* bonding. The values of the length for silicon–nitrogen bond when nitrogen is planar are about 0.07 Å shorter than our estimated value of 1.80 Å above. Both the planar geometry and the short bond length have been explained by assuming $d\pi$–$p\pi$ double bonding. The silicon–nitrogen *sigma* bond is formed by use of sp^2 hybrid orbitals on the nitrogen; the third (filled) *p* orbital on the nitrogen, oriented at right angles to the *sigma* bonding plane, overlaps with the empty *d* orbitals of the three attached silicons, forming delocalized *pi* bonds extending over all four atoms (Fig. 4). One would expect, as observed, that

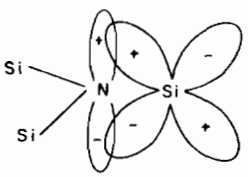

Fig. 4. Delocalized *pi* bond between filled nitrogen *p* orbital and silicon *d* orbitals extends over all four atoms.

the bonding situation described above would result in shorter bond lengths than anticipated for pure *sigma* bonding, because the introduction of *pi* character in the bond shortens the bond length.* It is worthy of mention here that the two silicon–nitrogen com-

*Some texts simply state that bonds formed from sp^2 hybrids are shorter than bonds formed from sp^3 because of less *p* influence in the hybridization, but since sp^2 cannot exist for nitrogen without *pi* character with the filled *p* orbital, the shortening is more accurately attributed to the latter reasoning.

pounds $(SiH_3)_3N$ and $(Si(CH_3)_3)_3N$ known to have planar nitrogen atoms have Si–N bond distances of 1.73 ± 0.01 Å and 1.74 ± 0.02 Å respectively.

It should also be noted that other elements (carbon, phosphorus, *etc.*) which have empty orbitals available for use in molecular orbitals of *pi* symmetry can cause a three-coordinate nitrogen with a filled *p* orbital to go planar. Perhaps the best-known example is the nitrogen in amides such as the peptide linkage in proteins, wherein the six atoms shown here

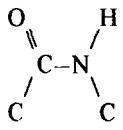

form a planar array.

(i) Beta *form*

Examination of the experimental data for β-Si_3N_4 reveals that there are two types of nitrogen atomic positions. For both types the nitrogen is essentially planar but the two types are easily distinguishable because of the difference in bond lengths. The species marked N(2) in Fig. 2 has three bonds of equal length, 1.745 Å, the longest bond observed in the *beta* form. These bonds will be considered as *sigma* bonds with least amount of *pi* character. The nitrogen labeled N(1) in Fig. 2 has two Si–N bond lengths (1.730 and 1.739 Å) which are significantly different from each other and both shorter than the Si–N(2) bonds. These two lengths apparently reflect different degrees of *pi* bonding.

The situation can be rationalized by analyzing the geometry which relates the *d* orbitals of Si to the three nitrogens with which it bonds. Take the z direction to be [001] and the x axis to be along [100], with silicon, tetrahedrally coordinated by *sigma* bonds, placed at the origin, as shown in Fig. 5.

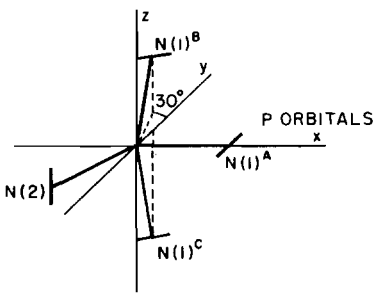

Fig. 5. The tetrahedrally coordinated silicon is at the origin. The lines through the nitrogen atoms depict the *p* orbitals perpendicular to the *sigma* bonding plane surround the nitrogens. These *d* orbitals enter into various degrees of *pi* bonding with silicon depending on their orientation with respect to the silicon *d* orbitals.

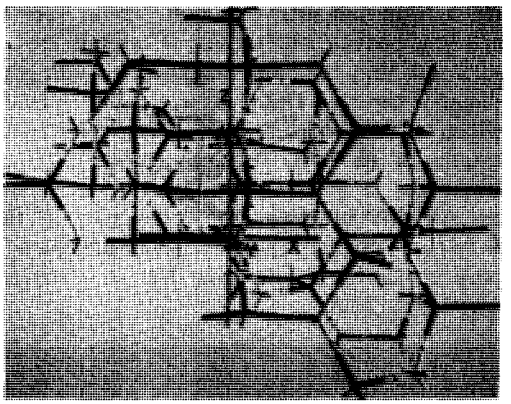

Fig. 6. Model of *beta* phase. Coordinate system labeled x, y, z. Black represents silicon. White represents nitrogen and metal prongs denote the filled *p* orbitals which enter into *pi* bonding with silicon *d* orbitals. Grey represents nitrogen but in this case the filled *p* orbitals are oriented so that only a small amount of *pi* bonding is possible. View of model such that coordination in Fig. 5 (above) is illustrated.

When a model of the *beta* structure (Fig. 6) is assembled, the orientation of the filled nitrogen *p* orbitals is seen to be as follows (schematically shown in Fig. 5): N(1)A along the [010] axis, N(1)B and N(1)C are 30° off the x axis in [1 $\sqrt{3}$ 0] and N(2) is on [001]. Since N(2) is not located on any {100} and since the filled *d* orbital is in the z direction, the Si *d* orbitals are oriented to allow only a small amount of *pi* bonding with N(2) using the silicon d_{zy} orbital. N(1)B and N(1)C, however, can form strong *pi* bonds with the d_{xz} and d_{yz} silicon orbitals and these would have a length less than that of the Si–N(2) bond which has less *pi* contribution. Finally the N(1)A can enter into a *pi* bond using the d_{xy} orbital of silicon but the overlap is not as great as that experienced by N(1)B and N(1)C but greater than with N(2) and consequently the N(1)A bond length will be intermediate between these other two bonds.

When this basic structure is repeated, as shown in the model (Figs. 1 and 6), one in every four nitrogens is seen to have the smallest *pi* bonding contribution. On the average, the other nitrogens are evenly divided between two bond lengths depending on the degree of *pi* bonding. Thus the three observed bond lengths (1.730, 1.739 and 1.745 Å) and two distinct nitrogen positions can be understood as a consequence of unequal *pi* overlap between the nitrogen and silicon.

(ii) Alpha *form*

The *alpha* structure is more difficult to analyze as a model with the observed bond lengths. In the *beta* form some of the nitrogen atoms had three bonds possessing the smallest amount of *pi* character because their unique *p* orbital, being oriented in the z direction, only allowed a little $p\pi$–$d\pi$ overlap. The

alpha form has nitrogens that exhibit very little *pi* bonding because their filled *p* orbitals are oriented such that they have negligible overlap with any of the silicon *d* orbitals. This leads to a structure (see Fig. 7) which can explain the heretofore enigmatic bond lengths of Table II. The absence of a 1.745 Å bond length (as in the *beta* form) is now understandable because the nitrogen (sp^2 hybridized in the *beta* form) with little *pi* character is replaced by an almost pure *sigma* bond and now has an observed bond length of 1.77 Å.

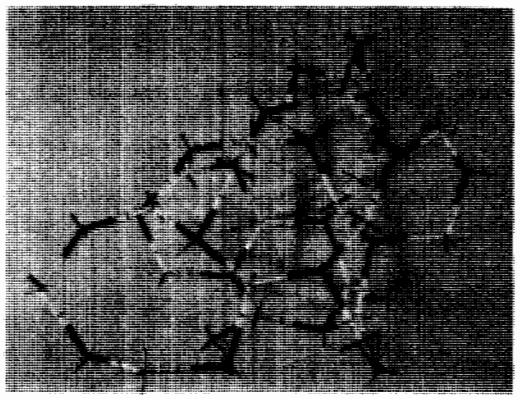

Fig. 7. A model of the *alpha* phase. Black represents silicon. White represents nitrogen. Grey denotes nitrogen which have entered into pure *sigma* bonds. Metal prongs on nitrogens without grey marker represent filled *p* orbitals which enter into *pi* bonding with silicon *d* orbitals. View looking down the z axis. The hexagonal building blocks can be seen in left hand section of this view.

Two families of silicon atoms appear in the *alpha* form, one next to the almost pure *sigma* bonded nitrogens and the other not so situated. If one defines a coordinate system for the *alpha* form in the same way as for the *beta*, the two families of silicon atomic sites can further be distinguished in the following way. Those silicons which do not have any almost pure *sigma* bonds to nitrogen form one of their Si–N *pi* bonds by overlap of their d_{z^2} orbitals with *p* orbitals of nitrogen which are suitably oriented. Cruikshank [19] predicts that this would be the strongest *p–d pi* bonding situation (see Fig. 8) for

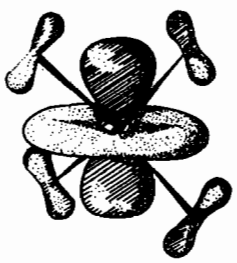

Fig. 8. Representation of *pi* bonding between d_{z^2} orbital and filled *p* orbitals (after Cruikshank [19]).

tetrahedrally coordinated silicon. Indeed such bonding could account for the unusually short (1.70 Å) Si–N bond length, which is observed only in the *alpha* structure.

Thus all of the observed bond lengths can be explained by postulating various degrees of *pi* bonding depending on the orientation of the nitrogen *p* orbitals relative to the silicon *d* orbitals. Furthermore, the large cavities (1.5 Å diameter) are bound by several nitrogens possessing almost pure *sigma* bonds. The oxygen of water (sometimes described as being in an sp^3 state) could easily substitute in place of these nitrogens in the *alpha* form, thus accounting for: 1) the formation of the *alpha* modification when water is present in the reaction atmosphere and 2) the high oxygen content repeatedly found in the *alpha* phase produced in some laboratories.

5. Examination of Microstructure

Because of its ceramic nature, silicon nitride is heterogeneous. A product must be characterized by a variety of tests. Densities (which reflect extent of reaction and amount of porosity) can be determined by measurement of sample volume and weight. A complete delineation of the microstructure – of great importance to any ceramic and especially to silicon nitride – can be obtained by a combination of powder X-ray diffraction analysis and optical, scanning electron (SEM) and transmission electron (TEM) microscopy. These are compared to such bulk properties as transverse rupture strength, creep and thermal shock resistance.

In view of the fact that at least three morphologies (*alpha* needles, *alpha* matte and *beta*) are present in silicon nitride samples, it is necessary to control microstructure by controlling some of the variables in the fabrication preparation process. Some of the data on preparation variables, reaction conditions and resultant predominant microstructural components are presented in Table III. Further data may be obtained by writing to the authors.

The chemical nature of ceramics is not often discussed in the inorganic chemistry literature; we feel therefore that some characteristic microstructural data is needed here before the discussion of formation mechanisms.

A. Alpha *Needles*

Alpha phase needles are commonly observed microconstituents. They grow in almost all samples but are particularly numerous in samples made from relatively impure silicon powder when some of the reaction is carried out at temperatures between 1350 and 1400 °C. Several features distinguish one type of needle from another but they are all characterized

TABLE III. Processing Parameters Encouraging Predominant Morphologies.[a]

Microconstituent	Time	Temperature	Heating Rate	Gas Flow Rate	Comment
α Needle	< 24 hr	< 1400 °C seems to favor needles	300 °C/hr	—	Observed in a majority of samples particularly less pure
β Blades	> 24 hr	> 1450 °C	—	—	Only observed when conditions are satisfied
α (fine) Matte	—	< 1450 °C	Slow	No Gas Flow	Use purer powder (finer)
β (coarse) Matte	> 5 hr	> 1450 °C	Rapid	Fast Gas Flow	
β Spikes	—	> 1450 °C	Rapid	Fast Gas Flow	Use less pure powder (coarser)
Large Pores	> 24 hr	> 1450 °C	Rapid	—	
Large Unreacted Grains	> 24 hr	< 1400 °C	300 °C/hr		

[a] — indicates that evidence collected thus far does not indicate variable is important.

by a high ratio of length to width (aspect ratio) around twenty-five.

Some needles, often having small beads on their ends, grow around larger silicon grains as shown in the SEM photograph of Fig. 9. They appear to have grown in the pores of the original compact. Other needles are found to be attached to either a large or small grain as shown in Fig. 10.

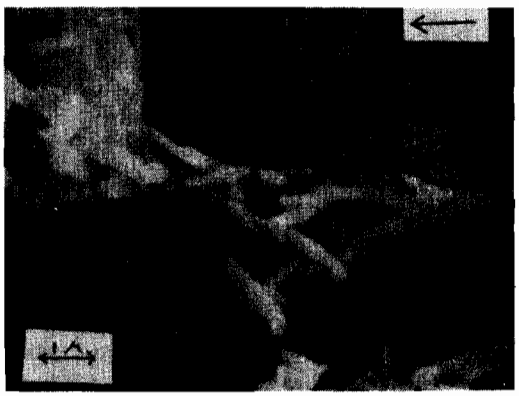

Fig. 9. Scanning electron micrograph of needles growing into original voidage of silicon compact. Some needles (A) are strongly anchored to larger grain (B), and other needles (C) grow independently of grains.

When examined in the transmission electron microscope there are two distinct types of needles. Some have a central core and an outer sheath which has no apparent structure and has been characterized by Evans and Sharpe [20] as being a crystalline core surrounded by an amorphous sheath. The other category of needles has lines running across them and these lines have been attributed to be interference bands, impurity bands, and dislocations. Both types of needles are shown in Fig. 11 as well as those having a bead at the tip.

Fig. 10. Scanning electron micrograph showing unreacted grain (A) being eaten away as needles form.

Fig. 11. Transmission electron micrograph showing different types of needles. (A) Needle with bead. (B) Needle with core and amorphous sheath. (C) Needle with markings.

B. Alpha *Matte*

The other major morphology of the *alpha* phase has been termed the *alpha* matte and is a fine grained structure. The conditions which favor the formation of this matte are slow heating of a sample to a temperature less than 1400 °C and no gas flowing over the sample.

In the early stages of formation the smallest silicon grains are the ones to react first and the product is often found around the larger grains particularly in areas where the grains were formerly contiguous (Fig. 12). The product is very fine grained ($< .5\mu$). As the

Fig. 12. Optical micrograph showing initial states of *alpha* matte (A) formation. Smallest grains react and fill in areas between larger grains (B). 1000X.

reaction proceeds all the smaller grains are consumed and the product fills the volume between larger grains. Porosity is introduced into these larger grains. Scanning electron micrographs show the matte advancing into grains with the characteristic porosity at the interface (Fig. 13). As time passes, nitridation to form the *alpha* phase matte comes to a stop before the large grains have completely reacted.

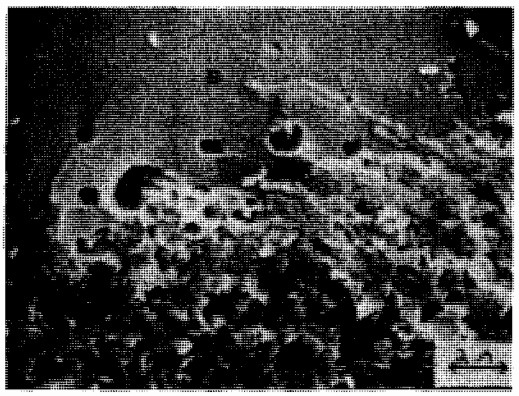

Fig. 13. Scanning electron micrograph of *alpha* matte (A) growing into grains (B) showing characteristic porosity at the interface. 5000X.

C. Beta *Phase*

The *beta* structure seems to predominate when a less pure sample of silicon (Table III) is heated rapidly in the presence of flowing nitrogen to a high temperature. In the initial stages of reaction the *beta* phase forms on the surface of a grain (Figs. 14 and 15), and spikes grow in towards the center of the

Fig. 14. Initial stages of *beta* phase (A) starting at surface and growing into grains (B). Optical 1000X. The *beta* phase appears as a smooth gray area.

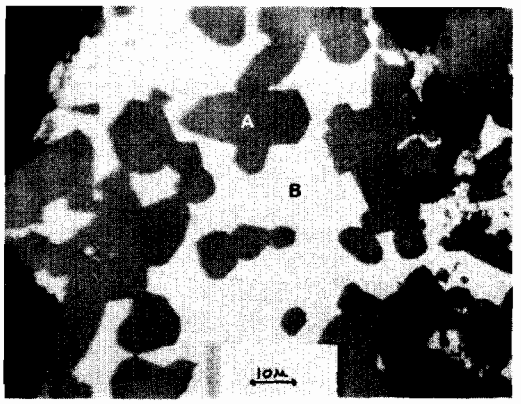

Fig. 15. Initial states of *beta* phase (A) showing cross section of grain (B) with spikes running through it. The spikes are growing in directions not in the plane of the photograph. Optical 1000X.

grain. The grain size is much larger than the size of *alpha* grains. As the reaction proceeds the spikes become larger and fill up more and more of the grain. Finally the spikes merge together in what appears to be one large reacted grain (Fig. 16).

If during this process, the temperature is raised and maintained well above the melting point of silicon (> 1500 °C) the silicon will melt and run out leaving cavities which allow scanning electron micrographs of the spikes to be obtained. Fig. 17 shows these spikes as they grow together into the grain.

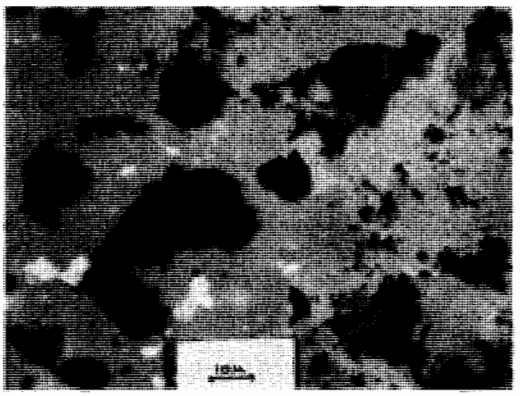

Fig. 16. Micrograph shows spikes that are in contact and appear to be one reacted grain. Optical 1000×.

Fig. 17. Fractograph showing spikes as they continue to grow and merge together. S.E.M. 2000×.

6. Macrostructure

A sample prepared by hot pressing or reaction bonding is polycrystalline. Despite the ease of formation of these aggregates, single crystals of either *alpha* or *beta* have been found to be difficult to grow and therefore have not been extensively studied. The major exception to this is a detailed optical microscopic study carried out by Clancy [21] in which polarized light was used to determine optic axis, principal indices of refraction, type of extinction and optic sign. Clancy points out the inherent danger in simply relying on X-ray diffraction analysis and states the necessity for further study of single crystals. Both the *alpha* and *beta* phases were observed to grow by both the vapor–liquid–solid and vapor–solid mechanisms. Growth direction and crystal habit are discussed in detail and it is observed that twins can form in either phase and that *beta* crystals have been observed to transfer either partially or completely into *alpha* crystals and *vice versa*.

An aggregate of crystals, however, forming either reaction-bonded or hot-pressed silicon nitride has been studied in some detail with particular attention being paid to properties of direct engineering significance (see Table IV). The bulk properties are dependent on microstructrure which, in turn, depends on processing conditions. A knowledge of this relationship is necessary to achieve an understanding of the formation mechanism which is invaluable when designing a material with specific properties.

The strength of reaction bonded silicon nitride is very dependent on such characteristics of the material as density and microstructure. Density is especially important because the degree to which a sample approaches the theoretical density of silicon nitride determines the number, size, and distribution of voids. These voids can act as microscopic flaws which in any brittle material limit the strength. Weibull statistics [22] have been used successfully in analyzing the strength of reaction bonded silicon nitride. Because there is no change in the bulk dimensions of the silicon compact during nitridation, the density and void size in the starting compact are very important in determining the physical properties of the reaction bonded material.

Fracture is always intergranular, *i.e.*, that the fracture path goes between the grains. At room temperature, a small grain size requires that the fracture path be irregular and more resistive to crack propagation and this means that a fine grained material will be stronger than a coarse grained material. In a ceramic the grains are stronger than the grain boundaries. This phenomenon may result from contamina-

TABLE IV. Properties of Silicon Nitride.

Property	Single Crystal	Hot Pressed	Reaction Bonded
Coefficient of Thermal Expansion	–	–	$2.5–3.2 \times 10^{-6}/C^{\circ}$
Density	α: 3.18 g/cc β: 3.19 g/cc	3.18 g/cc	2.2–2.8 g/cc
Modulus of Rupture	–	80–150 K.S.I.	13–50 K.S.I.
Knoop Hardness at 100 g load	–	900	1350

tion of the boundaries with impurity atoms or some second phase (especially a glassy phase). As chemists and engineers gain further understanding of the silicon nitride system the grain boundaries and consequently the bulk material can be made stronger. It should also be noted that grain size [23] has been related to high temperature creep rate, *i.e.*, the smaller the grain size the lower the creep rate which is contrary to the usual dependence.

As has already been mentioned, silicon nitride does not densify easily. In order to successfully hot press the material impurities are added (as densification aids, *e.g.*, magnesium oxide) and they tend to reduce the high temperature properties such as strength and creep resistance presumably by forming glassy grain boundary phases. Further development may improve the situation but even then the hot pressed material is expensive and difficult to fabricate into complex shapes.

7. Kinetics and Mechanism

A. Premise

It has been shown that there are two crystalline forms of silicon nitride and one of these exists in two distinct morphologies. It would be surprising if these forms of silicon nitride formed according to the same rate behavior and with the corresponding mechanism; in fact the overall kinetics of nitridation of silicon powder are complicated with both linear and logarithmic rates being reported [24]. It is our contention that the overall rate of reaction results from the superposition of (at least) two independent rate types with the various reaction conditions controlling the predominant mechanism for a single sample of ceramic.

B. Alpha *Needles*

In the section on *alpha* needle morphology above, an observation crucial to the formation mechanism was the bead seen at the tip of some needles. It was postulated that elemental silicon volatilized from the unreacted grains, was carried through the vapor phase to the bead which, at the temperature of reaction, probably is an impure liquid. Condensation of vapor inserts silicon into the liquid bead. Reaction therein with nitrogen adds solid silicon nitride to the elongating needle. As long as silicon can vaporize from the solid, as long as the bead remains liquid, and as long as nitrogen gas surrounds the bead, the needle will continue to grow in the direction of its long axis.

The energy barrier to *alpha* needle formation, provided no product coats the silicon surface, will be the solid-to-vapor transition because the covalent bonds that tie each silicon atom to the grain must be broken. The endothermicity of the process

$$Si_{(s)} \rightleftarrows Si_{(g)}$$

is about 86 kcal mol^{-1} The activation energy for vaporization should be about the same as the endothermicity. The condensation and crystallization steps probably will be exothermic so they should be more rapid. We presume that the breaking of the nitrogen–nitrogen bond can be accomplished in small steps so that this endothermicity can be offset by the simultaneous exothermic formation of silicon nitride.

Once the surface of the grains of silicon becomes coated with product, the slow step becomes complicated by diffusion of reactants through the nitride layer. The rate of product formation becomes slower as the layer of nitride thickens. For formation of *alpha* needles, silicon in some form must now diffuse through the layer and volatilize at the exterior of the product layer. It should be noted that oxygen contamination in the reaction atmosphere has been observed [25] to encourage the utilization of silicon by forming gaseous SiO. The introduction of oxygen can, therefore, increase the tendency to form *alpha* needles.

C. Alpha *Matte*

The *alpha* matte seems to be formed at the surface of the silicon particles, probably from the vapor phase. A detailed mechanism for the formation of *alpha* matte has been proposed by Atkinson *et al.* [25a]. Porosity is introduced into the silicon as a result of its diffusion through the nitride layer to reach the surface where it reacts with nitrogen. Assuming that the rate-controlling process now is diffusion of reactants (in opposite directions) through the nitride layer of *alpha* matte a first approximation of a rate law can be deduced [26] by the following consideration. The thickness of the diffusion layer will vary with time according to a law of the type

$$\frac{dy}{dt} = \frac{DK\Delta n}{y} \tag{1}$$

where y is the layer thickness, D is the diffusion coefficient (which will depend exponentially on temperature), K is a proportionality constant, and Δn is proportional to the driving force. This can be converted to the equation

$$(1 - \sqrt[3]{1 - x})^2 = \frac{DK't^{2/3}}{r^{5/3}} \tag{2}$$

where x is the % reacted, r is the particle radius, K′ is related to the above K plus a constant, and the constant D remains from above. This relation, similar to one developed by Jander [27], can be obtained from the physical situation that governs the "sintering" process when there is vapor phase transport: the radius of curvature of the "necks" joining

the particles is an integral part of the driving force (Δn) and it changes as the reaction proceeds and the neck thickens. Further work on this equation is necessary, but it will suffice for present purposes.

A comparison of the experimental values of % reaction of *alpha* phase with the predicted % based on this equation is shown in Fig. 18. The agreement is

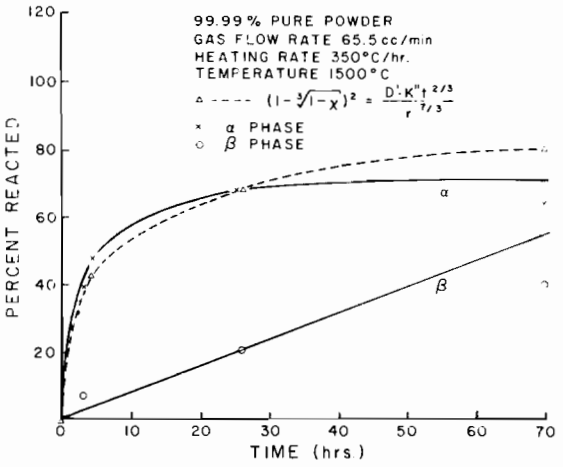

Fig. 18. The formation of *alpha* and *beta* phases obey two separate rate laws. The *beta* phase forms according to a linear rate law and the *alpha* phase forms according to a modified Jander rate law.

as good (supporting the concept that *alpha* Si_3N_4 comes from the vapor phase) as can be expected when one considers that each point represents a different experiment and that there are many critical processing conditions. Certainly there is a correlation between this theoretical relation and the rate of formation of the *alpha* phase.

D. Beta *Form*

Another important feature of Fig. 18 is that there are two separate and independent rates. The pattern for growth of the *beta* phase is very different from that of the *alpha*. The development and growth of the *beta* spikes in the silicon grains suggests that the product is formed at the inner tip of the spike. Nitrogen must adsorb on the surface and then diffuse down the hexagonal tunnels (see section on molecular structure) to the nitride–silicon interface.

The rate at which the *beta* phase forms and develops must depend on a number of conditions, including the probability of adsorption occurring (see below). This phase will continue to grow as long as room to expand (and therefore grow) inside a silicon grain allows (there is a 22% volume increase during reaction). Data from a few samples reacted under similar conditions indicate that the growth of the *beta* phase is linear at least when the reaction temperature is above the melting point of silicon.

E. Adsorption

It seems reasonable to hypothesize that adsorption of nitrogen gas onto the surface of solid silicon and silicon nitride is an important step in the formation of silicon nitride, particularly for the *beta* structure. If the nitrogen is to travel down the hexagonal tunnels previously described, it should first be adsorbed onto the surface and presumably preferentially to other gases (present as impurities). Since the entropy of adsorption should be negative because of loss of degrees of freedom (especially translational), the enthalpy would have to be negative (strong bonding to the surface) in order that the free energy of adsorption be negative (or at least near zero). This suggests that the N_2 is dissociated and forms strong bonds to atoms on the surface. There is some evidence that when nitrogen gas is adsorbed on a surface it can dissociate; this has been demonstrated [28] by the isotope scrambling

$$N^{15}N^{15} + N^{14}N^{14} \rightleftarrows 2N^{15}N^{14}$$

which has been found to occur on heterogeneous catalysts.

It is possible that, when a nitrogen molecule is adsorbed onto a *beta* silicon nitride surface, it undergoes scission. The small atoms may be drawn by capillary action into the hexagonal tunnels through which they apparently travel in order to reach the growth zone at the junction of product and reactant.

The step which would be slowest in the growth of *beta* spikes is difficult to assign. If it is adsorption combined with scission of the diatomic molecule, then the linear growth of *beta* is simply explained as a consequence of constant vapor-to-surface transfer. A constant rate of deposition of Si_3N_4 at the end of a spike in the silicon grain might also result in linear growth.

F. Degree of Reaction and the Alpha-*to*-Beta *Ratio*

The microscopic structures of ceramic silicon nitride leave little doubt that the growth of the *alpha* phase differs significantly in mechanism from that of the *beta* phase. The two competitive rates of product formation should have different (but not predictable) activation enthalpies and entropies. At any one temperature the kinetic competition will influence the relative amount of *alpha* and *beta* which will form. It appears to be the case that, at high temperatures and when impurities are present in silicon powder, the *beta* phase forms more rapidly than the *alpha* phase; at lower temperatures, the *alpha* phase seems to be kinetically favored. This implies that $\Delta H^{\neq}(\beta) > \Delta H^{\neq}(\alpha)$.

The very different mechanisms also suggest that the initial particle size of the silicon powder will be important in determining the product ratio; for smaller particle size we predict that a greater fraction of *alpha* will be formed. Smaller particles have a

higher surface-to-volume ratio and this when looked at in terms of the kinetics discussion above leads to the simple prediction. Furthermore the high radius of curvature and many "necks" joining particles will increase the driving force (Δn) as predicted by eqn. (2).

G. Beads on Surfaces

When a compacted silicon disc is heated rapidly in a nitrogen gas stream, small beads (silicon) often form on the surface of the reacting compact as shown in Figure 19. These beads react with the nitrogen gas to form small, flower-like arrays of crystallites as seen in Fig. 20. Apparently these beads (and possibly

Fig. 19. Unreacted beads on surface of sample.

Fig. 20. Reacted bead on surface of sample.

even the crystallites) also react with small amounts of oxygen and/or other oxygenated compounds. The composition of the bead reaction product was found to be a mixture of *alpha*-cristobalite, silicon oxynitride, silicon nitride and unreacted silicon. Conditions can be found where silicon nitride is the sole product.

Neither the physics nor the chemistry of bead formation or reaction is well understood, and further study is needed.

8. Summary of Conclusions

Silicon nitride is an important ceramic material, yet there remain a number of unresolved aspects of its chemistry. These have been mentioned in contexts above and are listed here. We reiterate them now in order to emphasize the need for its study by inorganic chemists.

(1) The solid samples have received little study of reaction with liquid water as functions of pH and temperature, and also with steam. The usefulness of an engine component depends greatly on its stability over a period of time under severe conditions.

(2) The thermodynamic measurements are complicated by a number of unresolved questions, not the least of which is that equilibrium among chemical components such as between the *alpha* and *beta* forms of Si_3N_4 has probably never been achieved.

(3) Single crystals of size large enough to carry out experiments on are hard to obtain. Even the whiskers seem to have a variety of domains.

(4) The importance of small amounts of impurities on chemical and physical properties is often mentioned yet remains as an important problem.

(5) More work on the relationships between sample preparation technique and chemical properties needs to be carried out.

Finally, we feel that control of particle size and reaction kinetics could lead to a material which would be largely in the *alpha* matte form, this being the modification that probably confers the greatest strength to a sample. In Fig. 72, shown is an optical micrograph of a silicon nitride sample made from milled silicon powder which has been reacted to give fine-grained *alpha* matte. A crystal of pure Si_3N_4 would have a density of 3.2 gm cc^{-1}, which indicates (when compared with the measured bulk densities) that the best reaction bonded samples made here have a porosity of about 28%. Fabrication practices are very critical in establishing the optimum properties of a sample. These practices are best understood if the inorganic chemist and the engineer have the relevant data; to date, this is not the case.

9. Acknowledgments

The authors would like to express their appreciation to the financial support of the U.S. Army Research Office (Durham) and to the optical and transmission electron metallography of Mr. Stephen C. Danforth and the technical assistance of Mr. Joseph Fogarty.

10. References

1 A. S. Berezhnoi, "Silicon and Its Binary Systems", Consultants Bureau, New York (1959).
2 *Badische Anilin und Soda Fabrik*, German Patent 224129, 29 (April, 1911).
3 A. Sinding-Larsen, U.S. Patent 928476, 20 (July, 1909).
4 Blix and Wirbelauer, *Ber., 36,* 4227 (1903).
5 E. Vigouroux, *Ann. Chim. Phys., 7,* 43 (1897).
6 L. Weiss and T. Engelhardt, *Z. Anorg. Chem., 65,* 38 (1910).
7 H. Funk, *Z. Anorg. Chem., 133,* 67 (1924).
8 E. Friederich and L. Sittig, *Z. Anorg. Chem., 134,* 293 (1925).
9 J. Collins and R. Gerby, *J. Metals, 1955,* 612 (1955).
10 N. Parr, Brit. Patent 974757 (1964).
11 U. Wannagat, *Adv. Inorg. Chem. and Radiochem., 6,* 255 (1964).
12 W. Croft and I. Cutler, "Review of Silicon Nitride", *E.R.P. Report No. 2-73, O.N.R. Report No. R-16-73* (July, 1973).
13 J. W. Edington, D. J. Rowcliffe and J. L. Henshall, *Powd. Met. Int., 7,* 82 (1975).
14 a) A. F. McLean, E. A. Fisher, R. J. Bratton and D. G. Miller, "Brittle Materials Design, High Temperature Gas Turbine", *A.M.M.R.C., CTR 75-8.* b) R. M. Horton, *J. Am. Ceram. Soc., 52,* 121 (1969). c) R. D. Pehlke and J. F. Elliot, *Tr. AIME 215,* 781 (1959). d) J. F. Elliot and M. Gleiser, "Thermochemistry for Steelmaking", vol. 1, Addison–Wesley, Reading, Mass., 1960. e) O. Kuboschewski and E. L. Evans, "Metallurgical Thermochemistry", Pergamon, London, 1958.
15 D. Messier and M. Murphy, "Silicon Nitride for Structural Applications – An Annotated Bibliography", *A.M.M.R.C. MS. 75-1* (Feb. 1975).
16 a) E. Turkdogan, P. M. Bills and V. Tippet, *J. Appl. Chem., 8,* 296 (1958). b) D. Hardie and K. Jack, *Nature, 180,* 332 (1957). c) I. Kohatsu and J. McCauley, "Re-examination of the Crystal Structure of α-Si_3N_4", *A.M.M.R.C. TR 74-25* (Oct. 1974). d) S. Wild, P. Grieveson and K. Jack, "Special Ceramics 5", Ed. P. Popper, The British Ceramic Research Association, 289 (1972).
17 H. S. Priest, S. C. Burns, G. L. Priest and E. C. Skaar, *J. Am. Ceram. Soc., 56,* 395 (1973).
18 K. Kijima, K. Kato, Z. Inouye and H. Tanaka, *J. Mat. Sci., 10,* 362 (1975).
19 D. Cruickshank, *J. Chem. Soc.,* 5486 (1961).
20 A. G. Evans and J. V. Sharp, "Electron Microscopy and Structure of Materials", G. Thomas, R. M. Fulrath and R. M. Fisher, Univ. of Calif. Press, 1972, p. 1141–1154.
21 W. Clancy, *The Microscope, 22,* 279 (1974).
22 D. Davies, *Proc. Brit. Ceram. Soc., 22,* 429 (1973).
23 A. McLean, E. Fisher and R. Bratton, *A.M.M.R.C. Interim Report Contract No. DAAG 46-71-C-0162,* July 1, 1973 thru Dec. 31, 1973.
24 D. Messier, P. Wong and A. Ingram, *J. Am. Ceram. Soc., 56,* 172 (1973).
25 a) D. Messier and P. Wong, "Kinetics of Fabrication of Silicon Nitride by Reaction Sintering", *Interim Report No. 1, A.M.M.R.C. TR 72-10* (March 1972). b) A. Atkinson, P. Leatt, A. Moulson and E. Roberts, *J. Mat. Sci., 9,* 981 (1974).
26 H. Jennings, "An Investigation of the Relationship between Processing Conditions, Microstructure and Mechanical Properties of Silicon Nitride", *Ph.D. Thesis,* Brown University (June 1975).
27 W. Kingery, "Introduction to Ceramics", Wiley, New York, 1960, p. 338.
28 H. Taylor, "The Solid Gas Interface", Ed. E. Flood, Marcel Dekker, New York, 1966, p. 1.